X-ray photoelectron spectroscopy of pyridinium-based tonic liquids: comparison to imidazolium- and pyrrolidinium-based analogues

ChemPubSoc Europe
DOI: 10.1002/cphc.201500227
CHEMPHYSCHEM Articles

X-ray Photoelectron Spectroscopy of Pyridinium-Based Ionic Liquids: Comparison to Imidazolium- and Pyrrolidinium-Based Analogues

Shuang Men,*[a, b] Daniel S. Mitchell,[b] Kevin R. J. Lovelock,[c] and Peter Licence*[b]

We investigate eight 1-alkylpyridinium-based ionic liquids of the form [C_nPy][A] by using X-ray photoelectron spectroscopy (XPS). The electronic environment of each element of the ionic liquids is analyzed. In particular, a reliable fitting model is developed for the C 1s region that applies to each of the ionic liquids. This model allows the accurate charge correction of binding energies and the determination of reliable and reproducible binding energies for each ionic liquid. Shake-up/off phenomena are determinedfor both C 1s and N 1s spectra. The electronic interaction between cations and anions is investigated for both simple ionic liquids and an example of an ionic-liquid mixture; the effect of the anion on the electronic environment of the cation is also explored. Throughout the study, a detailed comparison is made between [C_8Py][A] and analogues including 1-octyl-1-methylpyrrolidinium- ([C_8C_1Pyrr][A]), and 1-octyl-3-methylimidazolium- ([C_8C_1Im][A]) based samples, where X is common to all ionic liquids.

1. Introduction

The investigation of ionic liquids, which are organic salts with low melting points, has exhibited a dramatic growth over the past decade.[1] Since ionic liquids possess many fascinating and unique properties, such as very low vapour pressures, high thermal stability and excellent solvation properties, they have been under investigation with a great deal of interest for chemical synthesis, electrochemistry, lubrication and catalysis. To date, the majority of the research work, particularly in the fields of surface characterisation and ultra-high-vacuum (UHV) studies, has been mainly focused on imidazolium-[2] and pyrrolidinium-based ionic liquids.[3] Pyridinium-based ionic liquids have attracted more interest recently, mainly because of their proposed application in many processes, such as chemical reactions,[4] lubricant additives,[5] CO_2 capture[6] and fuel desulfurization.[7] They are considered as low-cost alternatives to imidazolium-based ionic liquids.[8] Compared to imidazolium-based ionic liquids, pyridinium-based ionic liquids exhibit better thermal stabilities,[9] higher viscosities,[7] slightly lower densities and similar surface tensions.[10] The excellent thermal stability is the huge advantage of pyridinium-based ionic liquids,[9,11] which also suggests that they may be investigated using a wide range of UHV techniques.

X-ray photoelectron spectroscopy (XPS) is now accepted as a reliable method for the characterisation of ionic-liquid-based systems.[2h] The focus of XPS studies is mainly the confirmation of the surface composition of ionic liquids and the identification of the electronic environments of certain elements present in the sample.[12] Binding energies, which give the experimentalist a measureable indicator of charge density, and hence charge distribution, can be easily determined for simple ionic liquids, mixtures and also for solutions, as long as the solute concentration is sufficient to be detectable by XPS.[2g,i–k,3a,13] In particular, cation–anion interactions of both simple ionic liquids and mixtures have been probed by using XPS.[2g,k,3a] These results have successfully been correlated with NMR spectroscopy[2g] and Kamlet–Taft parameters[2i,14] to aid in understanding the ionic liquid properties. Surface charging, as a result of the outgoing photoelectron flux, has been noted in the measurement of XP spectra of more viscous ionic liquids, and hence the development of robust fitting models and reliable charge-correction strategies has become essential to allow an inter-system comparison.[2i,j,3a]

In this study, we investigate eight 1-alkylpyridinium-based ionic liquids ([C_nPy][A]) by using XPS (see Table 1). We also investigate a mixture. A reliable fitting model is developed for the C 1s region of [C_nPy][A], which applies to all ionic liquids studied here—and that we believe will apply to all ionic liquids of this type. Shake-up/off phenomena are determined for both

[a] S. Men
School of Material Science and Engineering
Shenyang Ligong University
Shenyang 110168 (P. R. China)
E-mail: menshuang@hotmail.com
[b] S. Men, D. S. Mitchell, P. Licence
School of Chemistry
The University of Nottingham
Nottingham NG7 2RD (UK)
E-mail: peter.licence@nottingham.ac.uk
[c] K. R. J. Lovelock
Department of Chemistry
Imperial College London
London SW7 2AZ (UK)

Supporting Information for this article is available on the WWW under http://dx.doi.org/10.1002/cphc.201500227.

Table 1. Structure of the ionic liquids investigated in this study.

Abbreviation	Structure	Name
$[C_2Py][Tf_2N]$	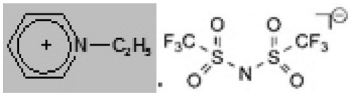	1-ethylpyridinium bis[(trifluoromethane)sulfonyl]imide
$[C_4Py][Tf_2N]$	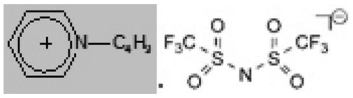	1-butylpyridinium bis[(trifluoromethane)sulfonyl]imide
$[C_6Py][Tf_2N]$	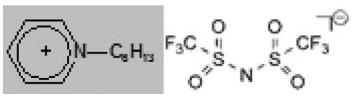	1-hexylpyridinium bis[(trifluoromethane)sulfonyl]imide
$[C_8Py][Tf_2N]$	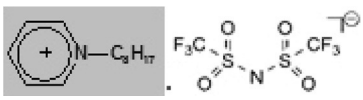	1-octylpyridinium bis[(trifluoromethane)sulfonyl]imide
$[C_{10}Py][Tf_2N]$	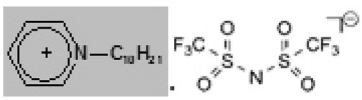	1-decylpyridinium bis[(trifluoromethane)sulfonyl]imide
$[C_{12}Py][Tf_2N]$	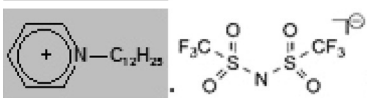	1-dodecylpyridinium bis[(trifluoromethane)sulfonyl]imide
$[C_8Py]Br$	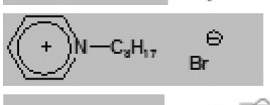	1-octylpyridinium bromide
$[C_8Py][PF_6]$	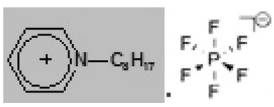	1-octylpyridinium hexafluorophosphate
$[C_8C_1Pyrr][Tf_2N]$	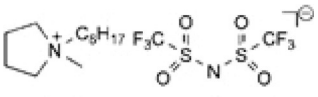	1-octyl-1-methylpyrrolidinium bis[(trifluoromethane)sulfonyl]imide
$[C_8C_1Im][Tf_2N]$	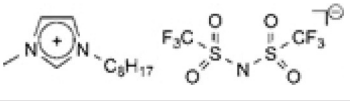	1-octyl-3-methylimidazolium bis[(trifluoromethane)sulfonyl]imide

C 1s and N 1s spectra. Cation–anion interactions are investigated for both simple ionic liquids and an ionic liquid mixture; the effect of the anions on the electronic environment of the cation is explored in detail. Throughout the study, comparisons are made to imidazolium-based and pyrrolidinium-based ionic liquids. In particular, a detailed comparison is made between $[C_8Py][A]$ and 1-octyl-3-methylimidazolium ($[C_8C_1Im][A]$) and 1-octyl-1-methylpyrrolidinium ($[C_8C_1Pyrr][A]$) based analogues, where A is common for all samples.

Experimental Section

Materials

All chemicals were obtained from Sigma–Aldrich or Alfa Aesar and were used as received. Lithium *bis*[(trifluoromethane)sulfonyl]imide (3 M) was used as received. All the ionic liquids investigated herein were prepared following established synthetic protocols, $[C_8Py]Br$,[15] $[C_8Py][PF_6]$,[15] $[C_nPy][Tf_2N]$,[8a] where $n = 2$, 4, 6, 8, 10 and 12. The structures of the individual cations and anions investigated in this study are shown in Table 1.

Unless otherwise stated, all ionic liquids were characterised by ^1H and ^{13}C NMR spectroscopy. The spectra were recorded on a Bruker DPX-300 spectrometer at 300 and 75 MHz, respectively, as solutions in $CDCl_3$ or $[D_6]DMSO$. If anion exchange was one of the synthetic steps, ion chromatography showed that the halide concentration was < 10 ppm. No halide signal was observed by XPS analysis, that is, the concentration was below the limit of detection in every case. Full data for all the materials studied in this work appears in the Supporting Information.

XPS Data Collection

All XP spectra were recorded using a Kratos Axis Ultra spectrometer employing a focused, monochromated Al Kα source ($h\nu = 1486.6$ eV), hybrid (magnetic/electrostatic) optics, hemispherical analyser and a multi-channel plate and delay line detector (DLD) with an X-ray incident angle of 30° and a collection angle of 0° (both relative to the surface normal). The X-ray gun power was set to 100 W. All spectra were recorded using an entrance aperture of 300×700 μm with a pass energy of 80 eV for survey spectra and 20 eV for high-resolution spectra. The instrument sensitivity was 7.5×10^5 counts s^{-1} when measuring the Ag $3d_{5/2}$ photoemission peak for a clean Ag sample recorded at a pass energy of 20 eV and 450 W emission power. Ag $3d_{5/2}$ full-width-half-maximum (FWHM) was 0.55 eV for the same instrument settings. Binding-energy calibration was made using Au $4f_{7/2}$ (83.96 eV), Ag $3d_{5/2}$ (368.21 eV)

and Cu $2p_{3/2}$ (932.62 eV). The absolute error in the acquisition of binding energies was ± 0.1 eV, as quoted by the instrument's manufacturer (Kratos). Consequently, any binding energies within 0.2 eV can be considered the same, within the experimental error. Charge neutralisation methods were not required (or employed) in the measurement of these data. Sample stubs were earthed ***via*** the instrument stage using a standard BNC connector.

Samples were prepared by placing a small drop ($\approx$20 mg) of the ionic liquid into a depression on a stainless-steel sample stub (designed for powders) or on a standard stainless-steel multi-sample bar (both Kratos designs). The ionic-liquid samples were presented as thin films (approx. thickness 0.5–1 mm), thereby avoiding experimental complications associated with variable sample height. Initial pumping to high-vacuum pressure was carried out in a preparation chamber immediately after thin film preparation to avoid significant absorption of volatile impurities. Pumping of ionic liquids was carried out with care as the high viscosities associated with these samples meant that significant bubbling due to removal of volatile impurities was observed. The pumping down process was consequently carried out slowly to avoid contamination of the UHV chamber by bumping/splashing of the ionic liquid samples. The preparation chamber pressure achieved was $\approx 10^{-7}$ mbar. Pumping times varied (1–3 hrs total) depending upon the volume, volatile impurity content and viscosity of the sample, that is, viscous ionic liquids were found to require longer pumping times. The samples were then transferred to the main analytical vacuum chamber. The pressure in the main chamber remained $\leq 1\times10^{-8}$ mbar during all XPS measurements, suggesting that all volatile impurities, such as water, were removed, leading to high-purity samples.[16] For clarity, a full description of the data analysis is included below; full experimental details and a discussion of a modified fitting procedure are also included.

Information Depth of XPS

The information depth (ID) of the XPS experiments may be defined as the depth, within the sample, from which 95% of the measured signal will originate. The ID is assumed to vary mainly with the cos θ, where θ is the electron emission angle relative to the surface normal. If we assume that the inelastic mean free path (λ) of photoelectrons in organic compounds is of the order of ~3 nm, at the kinetic energies employed here, we can estimate the ID in this geometry. If $\theta = 0^\circ$, ID = 7–9 nm. Consequently, these data may be considered as representative of the bulk composition and do not reflect any local enhancements of concentration near the surface.

XPS Data Analysis

For data interpretation, a two point linear background subtraction was used; for $[Tf_2N]$-based ionic liquids, the C 1s XP spectra were subtracted using a linear spline to allow for the CF_3 substituent. Peaks were fitted using GL(30) lineshapes; a combination of a Gaussian (70%) and Lorentzian (30%).[17] This lineshape has been used consistently in the fitting of XP spectra, and has been found to match experimental lineshapes for ionic-liquid systems.[2i, 3a] The FWHM of each component was initially constrained to $0.8 \leq$ FWHM ≤ 1.5 eV. All XP spectra where $n = 8$ were charge-corrected by setting the binding energy of the aliphatic C 1s photoemission peak ($C_{aliphatic}$ 1 s) equal to 285.0 eV. For all the other values of n (i.e. when $n = 2$, 4, 6, 10 and 12), the spectra were charge-corrected by setting the measured binding energy of the cationic nitrogen photoemission peak (N_{cation} 1 s) equal to 402.6 eV.[2g, i, 3a, 12a, 18] Relative sensitivity factors (RSF) were taken from the Kratos Library (RSF of F 1s = 1) and were used to determine the atomic percentages.[19] It should be noted that there was no evidence of either Li or halide contamination carried over from ion-exchange chemistries employed in synthesis, or additional hydrocarbon/oxygen impurities in the XP spectra of any of the ionic liquids studied herein. The experimental stoichiometries, determined from high-resolution XP spectra for each of the ionic liquids studied herein, were within the experimental error of nominal stoichiometries determined from the empirical formulae of the sample.

2. Results and Discussion

2.1. The Electronic Environment of Carbon: Fitting Model

The C 1s XP spectra of $[C_nPy][Tf_2N]$ are generally characterised by two distinct photoemission envelopes. The largest one appears to be composed of at least three identifiable contributions, which can be identified as distinct sets of contributions from the C atoms nearest to the charge carrier, that is, three different chemical environments within the pyridinium ring. The first component, C_{hetero}, is the carbon bonded to nitrogen; all $[C_nPy]^+$ contain three such atoms, labelled ($C^2 + C^6 + C^7$). The second component, C_{inter}, corresponds to the remaining three carbons within the pyridinium head group, labelled ($C^3 + C^4 + C^5$), the final and largest component, $C_{aliphatic}$, corresponds to the sp^3 hybridised carbon that is bonded to carbon and hydrogen only; the size of this component varies depending on the magnitude of n (see Figure 1 a $[C_8Py][Tf_2N]$ as an example).

It must be noted that the shake-up/off phenomenon is more pronounced in the carbon (taking $[C_8Py][Tf_2N]$ as an example, see Figure 1 a) and nitrogen regions (see Figure 1 b) for pyridinium-based ionic liquids. The observation of a shake-up satellite is due to the π–π^* excitation of a valence electron after the photoemission involved in multiple bonding and/or aromatic compounds.[17, 20] During this process, the photoelec-

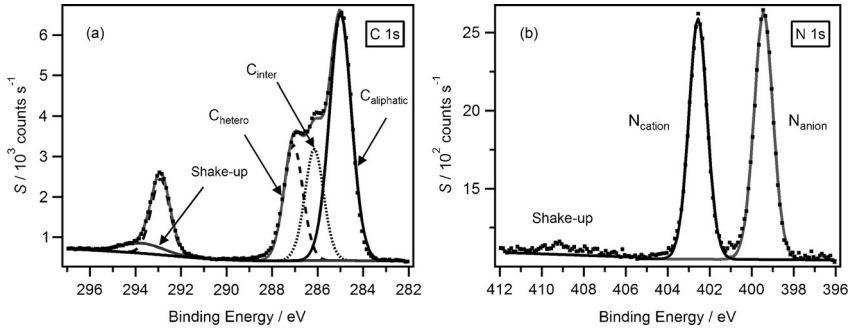

Figure 1. a) C 1s and b) N 1s XP spectra with component fittings and shake-up of $[C_8Py][Tf_2N]$. All XP spectra were charge-corrected by referencing the aliphatic C 1s component ($C_{aliphatic}$ 1 s) to 285.0 eV.

tron will lose some of its kinetic energy, and thus shows a higher binding energy. Moreover, in a process similar to a 'shake up', the valence electrons can be completely ionised, that is, excited into an unbound continuum state. This 'shake-off' process will leave an ion with vacancies in both the core level and the valence band. During the 'shake-off' process, no apparent signal will be observed, as the photoelectron will lose most of its kinetic energy and thus contribute to the inelastic baseline.[21] Shake-off occurs parallel to the shake-up process.[22] Both shake-up and shake-off result in an intensity loss of the main photoemission peaks of 5–20%.[23] The percentage of intensity loss depends on both the element and the chemical environment itself.[24]

For $[C_8C_1Im][Tf_2N]$, shake-up/off is obscured by the more intense signal from the photoelectrons of the -CF_3 group[2i] (see Figure S10). For $[C_8C_1Pyrr][Tf_2N]$, no shake-up/off phenomenon could be observed, as there is no multiple-bond character present, and therefore, the positive charge is localised only on the nitrogen atom (see Figure S11). For $[C_8Py][Tf_2N]$, it is apparent that a shoulder can be observed, which overlaps with the signal from the -CF_3 group (Figure 1a). The shake-up/off reduction was determined for a series of pyridinium-based ionic liquids in this study, see Table 2. An average value of 10% was used to describe the shake-up/off losses and ensured that the area ratios of the components in the C1s fitting model were accurate.

Table 2. Shake-up/off of C1s and N1s photoelectron losses compared to all carbon and nitrogen atoms within the pyridinium headgroup, respectively.

Cation	Anion	Shake-up/off % per Py C atom	Shake-up/off % per Py N atom
$[C_2Py]^+$	$[Tf_2N]^-$	12.3	9.7
$[C_4Py]^+$	$[Tf_2N]^-$	10.9	10.0
$[C_6Py]^+$	$[Tf_2N]^-$	9.7	10.2
$[C_8Py]^+$	$[Tf_2N]^-$	10.0	9.8
$[C_{10}Py]^+$	$[Tf_2N]^-$	9.3	8.4
$[C_{12}Py]^+$	$[Tf_2N]^-$	10.3	9.7
$[C_8Py]^+$	$[PF_6]^-$	8.5	5.7
$[C_8Py]^+$	Br^-	9.7	8.4
Average		10.1	9.0

Taking into account the 10% shake-up/off loss, it is finally concluded that the area ratios of the three $[C_nPy]^+$-based components were constrained to $C_{hetero}:C_{inter}:C_{aliphatic} = 2.8:2.7:(n\text{-}1)$, when $n = 2$–12. The FWHM of C_{hetero} and C_{inter} were constrained to be equal to each other. It should be noted that the FWHM ratio of ($C_{aliphatic}$ 1s):(C_{hetero} 1s) was 1.08, when $n = 2$–12, which illustrates that all carbon atoms labelled as $C_{aliphatic}$ are in very similar environments. Application of these constraints gave rise to a satisfactory fit when $n = 2$–12.

For $[C_8Py][PF_6]$ (see Figure S7) and $[C_8Py]Br$ (see Figure S8), three $[C_nPy]^+$ components were also employed, although only two distinct peaks could be observed for $[C_8Py]Br$. The key assumption for a satisfactory three-component fitting model was that the FWHM ratio of ($C_{aliphatic}$ 1s):(C_{hetero} 1s) was 1.08, as determined for $[C_nPy][Tf_2N]$, where $n = 2$–12 (see Figure S1–S6).

2.2. The Electronic Environment of Nitrogen and Other Anion Regions

The N1s XP spectra of $[C_nPy][Tf_2N]$, where $n = 2$–12, contain two peaks (Figure 2), whereas the N1s XP spectra of $[C_8Py][PF_6]$ and $[C_8Py]Br$ both contain one peak only (see Figures S7 and S8). The peak at higher binding energies, that is, 402.4 to 402.7 eV, can therefore be assigned to the nitrogen atom from

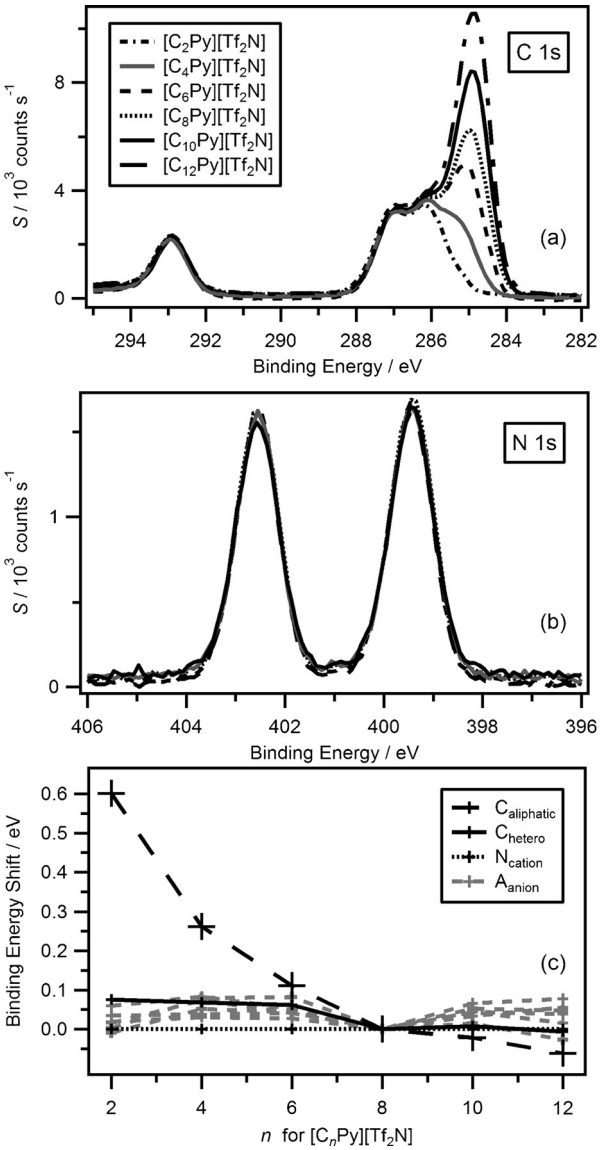

Figure 2. XP spectra for $[C_nPy][Tf_2N]$ where $n = 2$–12 for: a) C1s, b) N1s. The intensities are normalised to the intensity of the N_{cation} 1s fitted peak for $[C_8Py][Tf_2N]$. For $n = 8$, the XP spectra were charge-corrected by referencing the aliphatic C1s component ($C_{aliphatic}$ 1s) to 285.0 eV. For other n values, the XP spectra were charge-corrected by referencing the N_{cation} 1s to the value for $n = 8$. c) Binding energy shifts relative to $[C_8Py][Tf_2N]$ as a function of the aliphatic chain length, $n = 2$–12. It should be noted that the experimental error associated with the measurement of binding energies is of the order ±0.1 eV.

the pyridinium headgroup, and is labelled N_{cation} 1s. The peak at lower binding energy for $[C_nPy][Tf_2N]$, ~399.5 eV, can be assigned to the nitrogen atom from the $[Tf_2N]^-$ anion, labelled N_{anion}, as assigned previously for $[C_nC_1Im][Tf_2N]$ and $[C_nC_1Pyrr][Tf_2N]$ ionic liquids.[2i, 3a, 18, 25] As the binding energy of N_{cation} 1s is far greater than that of N_{anion} 1s, the nitrogen atom of the pyridinium cation is more electropositive than the nitrogen atom of the $[Tf_2N]^-$ anion. The peak intensity ratio is ~0.9:1 for all $[C_nPy][Tf_2N]$ ionic liquids, considering the shake-up/off loss.

The fluorine, oxygen and sulfur regions of $[C_nPy][Tf_2N]$ all show one electronic environment, as expected based on previous XPS studies of $[C_nC_1Im][Tf_2N]$ and $[C_nC_1Pyrr][Tf_2N]$ (see Figures S1 to S6).[2i, 3a] The six fluorine atoms are indistinguishable by XPS, and the same is true for the four oxygen atoms and two sulfur atoms. It must be noted that the observed double-peak structure of the S 2p level is due to spin-orbit splitting into the $S\,2p_{1/2}$ and $S\,2p_{3/2}$ levels (in a ratio of 1:2). For $[C_8Py][PF_6]$, the F 1s XP spectrum gives a single peak, showing that all six fluorine atoms are indistinguishable by XPS (see Figure S4). The P 2p spectrum shows two peaks due to the spin-orbit splitting, and only one phosphorus electronic environment was observed. For $[C_8Py]Br$, the Br 3d spectrum shows two peaks in a ratio of 2:3; these peaks are also due to the spin-orbit splitting (see Figure S8). Therefore, there is only one bromide electronic environment present, as expected.

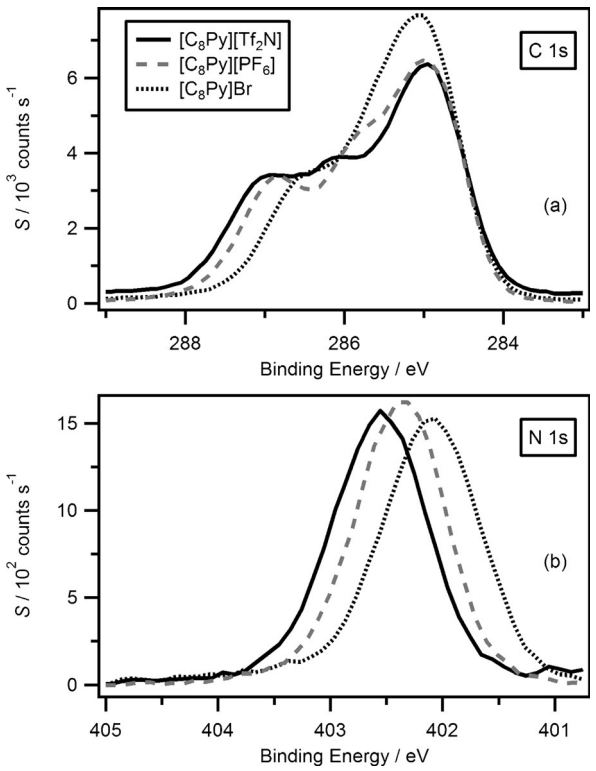

Figure 3. XP spectra for $[C_8Py][Tf_2N]$, $[C_8Py][PF_6]$ and $[C_8Py]Br$ of a) C 1s, b) N 1s. The intensities are normalised to the intensity of the N_{cation} 1s fitted peak for $[C_8Py][Tf_2N]$. All the XP spectra were charge-corrected by referencing the aliphatic C 1s component ($C_{aliphatic}$ 1s) to 285.0 eV.

2.3. Measurement of Accurate Binding Energies and the Effect of the Aliphatic Chain Length on the Binding Energies

In the previous section, we described the development of a reliable fitting model for the C 1s region of ionic liquids of general formula $[C_nPy][A]$. The binding energies obtained for the $C_{aliphatic}$ 1s component of this fit can be used as an internal charge referencing by setting the observed $C_{aliphatic}$ 1s component equal to 285.0 eV for $[C_8Py][A]$. All other regions are subsequently shifted by the same amount as the $C_{aliphatic}$ 1s component. The binding energy of N_{cation} 1s for $n=8$ (402.6 eV) can then be used to charge-correct all $[C_nPy][A]$ ionic liquids, where $n=2$, 4, 6, 10 and 12, as the electronic environment of N_{cation} is not expected to vary with n, as long as $[A]^-$ is unchanged. Figures 2a and 2b show the charge-corrected C1s and N 1s XP spectra for $[C_nPy][Tf_2N]$. All the binding energies remain constant as n varies, apart from the $C_{aliphatic}$ 1s component (Figure 2c). The conclusion is that the length of the aliphatic chain makes little or no difference to the interaction of the charged moieties of the cation and anion, and therefore, to their electronic interaction. For $n=6$, 8, 10 and 12, the binding energies of $C_{aliphatic}$ are the same, within the error of the experiment. This observation shows that the $C_{aliphatic}$ component for these ionic liquids is a good representation of aliphatic carbon. For $n=4$, clearly the binding energy of the $C_{aliphatic}$ 1s component increases significantly relative to $n=8$, indicating that the three aliphatic carbons for $[C_4Py][Tf_2N]$ are much more electropositive than the aliphatic carbon atoms further away from the nitrogen atom. For $n=2$, as the only aliphatic carbon is bonded β to the nitrogen atom within the cation headgroup, it is obvious that this carbon is more electron-poor and therefore shows a higher binding energy. This difference is due to the relative distance of the carbon atoms from the electropositive nitrogen atom. Therefore, $C_{aliphatic}$ 1s for $n=2$ and 4 cannot be used for satisfactory charge correction, whereas $C_{aliphatic}$ 1s for $n\geq 6$ can be used. Throughout this contribution, the binding energy of $C_{aliphatic}$ 1s for $n=8$ was set to 285.0 eV. As the binding energy for N_{cation} 1s is unaffected by n, this value (402.6 eV) was used for charge correction of $[C_nPy][Tf_2N]$, where $n=2$, 4, 6, 10 and 12. This procedure has been shown to be robust for all families of ionic liquids when the alkyl substituents on the charge carriers are large (i.e. when $n\geq 8$).[2i,j, 3a, 14] All charge-corrected binding energies are presented in Table S1.

2.4. Simple $[C_8Py][A]$ Based Ionic Liquids and Ionic-Liquid Mixtures

Previous studies have suggested that cation–anion interactions can be investigated by XPS.[2g,j,k, 3a] The binding energies of C_{hetero} 1s and N_{cation} 1s have been shown to correlate with the anion basicity. For low-basicity anions such as $[Tf_2N]^-$, the binding energies are relatively high, meaning that the cation is relatively electropositive. Clearly, low-basicity anions transfer less charge to the cation; the opposite is true for high-basicity anions such as Cl^-, Br^- and $[OAc]^-$.

The effect of the anion on the charge transferred to the cation has been investigated for three $[C_8Py][A]$ ionic liquids,

where $[A]^- = [Tf_2N]^-$, $[PF_6]^-$ and Br^- (Figure 3). The binding energies of the N 1s and C 1s XP spectra are charge-corrected to $C_{aliphatic}$ 1s = 285.0 eV. The areas are normalised to the area of N_{cation} 1s. The binding energies for both N_{cation} 1s and C_{hetero} 1s follow the trend: $[Tf_2N]^- > [PF_6]^- > Br^-$. The higher binding energy corresponds to a more electropositive cation. Therefore, more charge is transferred from the anion to the cation for the more basic anion, Br^-. These results are in agreement with those for imidazolium-[2g,j] and pyrrolidinium-based ionic liquids.[3a]

Mixtures of ionic liquids have previously been studied by using XPS to investigate both surface composition[26] and binding energy shifts.[2k, 3a]

A 1:1 mixture of $[C_8Py][Tf_2N]$:$[C_8Py]Br$ was chosen because firstly the simple ionic liquids have been studied, and secondly, the anions have relatively different basicities. The differences in basicity for the two anions are sufficiently large so that the differences in binding energies of C_{hetero} 1s and N_{cation} 1s are larger than the magnitude of the error of the experiment. The same cation was chosen to keep the number of variables at a minimum and enable relatively simple and accurate charge referencing. The XP spectra for C 1s, N 1s and Br $3d_{5/2}$ are given in Figure 4. The binding energies of C_{hetero} 1s and N_{cation} 1s for the mixture are different to those of the simple ionic liquids, in between those for the two simple ionic liquids (Figures 4a and 4b). However, the peaks for N_{anion} 1s and Br $3d_{5/2}$ show no binding energy deviations for the mixture from the simple ionic liquids (Figures 4b and 4c). These results show that the electronic environment of the cation can be tuned to a desired value by varying the amounts of different anions. However, within the error of the experiment, one anion has no effect on another anion, if the cation is the same. It is vital to point out that the FWHM of N_{cation} 1s for the mixture is similar to that for the simple ionic liquids. This observation demonstrates that for the mixture, the cation is in one electronic environment, not a mixture of two electronic environments (such a scenario would likely give rise to a single peak with a significantly larger FWHM than those of the simple ionic liquids). The conclusion is that the ionic liquid mixture contains intimate mixtures of cations and the different anions, not pockets of the cation and one type of anion, with other pockets of the cation and the other anion. These results agree with those obtained for pyrrolidinium-based ionic liquids.[3a]

Overall the results for both simple $[C_8Py][A]$ and the mixture show that the anion can significantly influence the electronic environment of the cation. This knowledge can be used to tune the electronic environment of the cation, in particular by selection of anions and using the appropriate mixture.

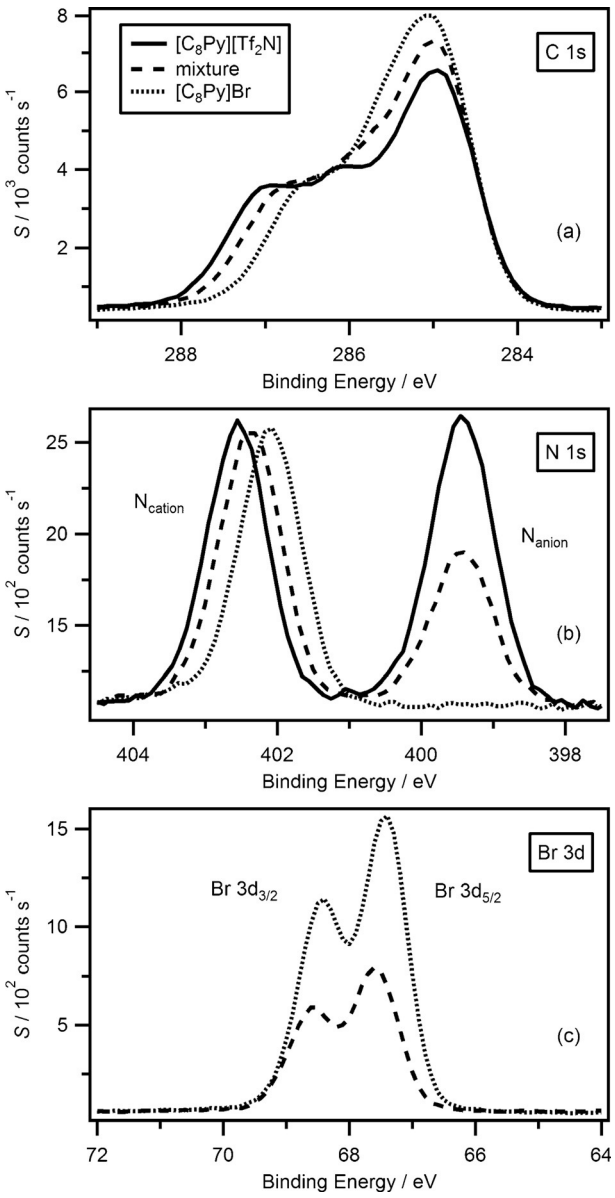

Figure 4. C 1s, N 1s and Br 3d for a 1:1 $[C_8Py][A]$ mixture of $[C_8Py][Tf_2N]$ and $[C_8Py]Br$. The intensities are normalised to the intensity of the N_{cation} 1s fitted peak for $[C_8Py][Tf_2N]$. All the XP spectra were charge-corrected by referencing the aliphatic C 1s component ($C_{aliphatic}$ 1s) to 285.0 eV.

2.5. Comparison of $[C_8Py][A]$ versus $[C_8C_1Pyrr][A]$ and $[C_8C_1Im][A]$

Comparisons can now be made amongst binding energies of pyridinium-based ionic liquids, pyrrolidinium-based ionic liquids and imidazolium-based ionic liquids. A visual comparison of $[C_8Py][Tf_2N]$, $[C_8C_1Pyrr][Tf_2N]$ and $[C_8C_1Im][Tf_2N]$ for all regions is given in Figure 5. The XP spectra are all charge-corrected to the binding energy of $C_{aliphatic}$ 1s, and are normalised to the area of the F 1s peak, as all ionic liquids contain six fluorine atoms. The first observation is that the relative areas of the components agree well, for example, S 2p, O 1s, C_{CF3} 1s, N_{anion} 1s, confirming the validity of normalising the areas of the XP spectra. The second, more important, observation is that the binding energies of all the anion components match, within the error of the experiment (Figures 5a–e and Table S1). For example, F 1s for $[C_8Py][Tf_2N]$ is 688.8 eV, and for $[C_8C_1Pyrr][Tf_2N]$ and $[C_8C_1Im][Tf_2N]$ 688.9 eV and 688.8 eV, respectively. In addition, for $[C_8Py][PF_6]$, $[C_8C_1Pyrr][PF_6]$ and $[C_8C_1Im][PF_6]$, the binding energies of the P $2p_{3/2}$ and F 1s components are the same (136.6 eV and 686.6/686.6/686.7 eV, respectively, see Table S1).

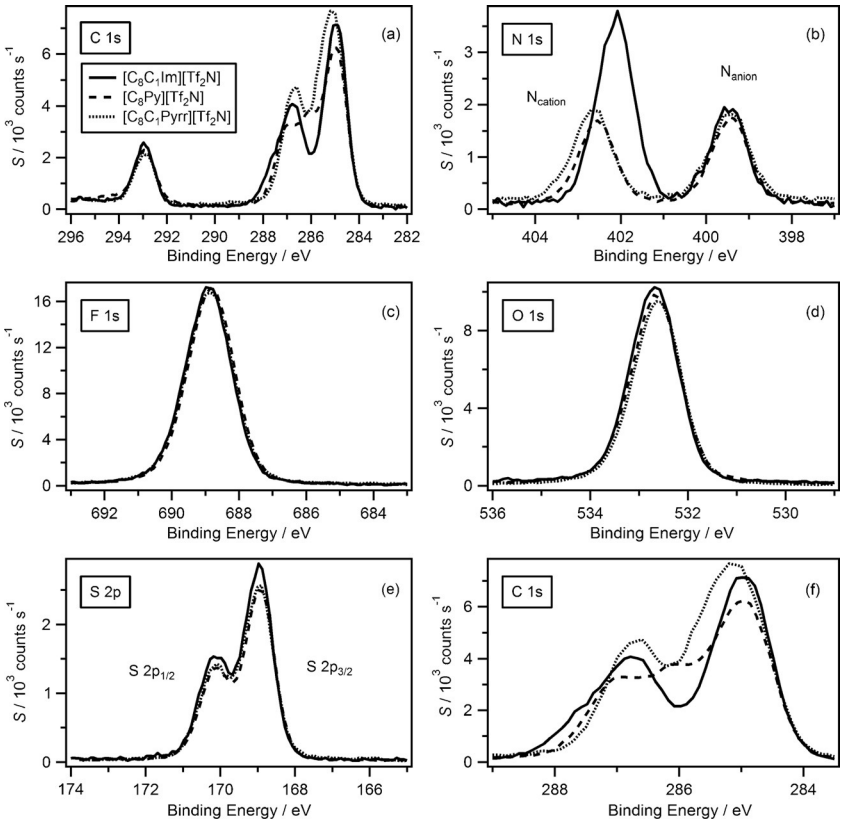

Figure 5. XP spectra of $[C_8Py][Tf_2N]$, $[C_8C_1Pyrr][Tf_2N]$ and $[C_8C_1Im][Tf_2N]$ for: a) C 1s, b) N 1s, c) F 1s, d) O 1s, e) S 2p and f) C 1s with chopped *x* axis. The intensities are normalised to the intensity of the F 1s peak for $[C_8Py][Tf_2N]$. All the XP spectra were charge-corrected by referencing the aliphatic C 1s component ($C_{aliphatic}$ 1s) to 285.0 eV.

These observations indicate that changing the cation of the ionic liquid has relatively little effect on the electronic environment of the anion.

However, there are significant differences in spectra when comparing the binding energies of the peaks derived from the cations, see Figures 5a and 5b. The binding energy of the N_{cation} 1s for $[C_8Py][Tf_2N]$ is 402.6 eV, which is the same as that obtained for $[C_8C_1Pyrr][Tf_2N]$ (402.7 eV), within the experimental error, but different from that obtained for $[C_8C_1Im][Tf_2N]$ (402.1 eV). In general, the N_{cation} 1s binding energies for $[C_8Py][A]$ and $[C_8C_1Pyrr][A]$ are higher than those for $[C_8C_1Im][A]$ (0.5 ± 0.1 eV) when $[A]^-$ is the same, see Table S1. The nitrogen atom in $[C_8C_1Pyrr][A]$ is in sp^3 hybridisation whereas it is in sp^2 hybridisation in the cases of $[C_8Py][A]$ and $[C_8C_1Im][A]$. The similar binding energies measured for $[C_8C_1Pyrr][Tf_2N]$ and $[C_8Py][Tf_2N]$ indicate that the nitrogen atoms, regarding hybridisation, are still in similar partial-charge environments. Since there are two nitrogen atoms within the imidazolium cation headgroup, the partial positive charge over each atom is lower, which gives rise to a noticeably higher electron density at each atom, and thus to a lower binding energy. The binding energies of the carbon atoms within the cations can also be compared. It is evident that $[C_8C_1Im][Tf_2N]$ contains a cation-based C 1s component with a higher binding energy than those observed for $[C_8C_1Pyrr][Tf_2N]$ and $[C_8Py][Tf_2N]$ (Figures 5a and 5f). This component for $[C_nC_1Im][A]$ has been identified as the carbon within the imidazolium cation that is bonded to two nitrogen atoms, that is, at the C^2 position.[2i,12a] The C^2 atom of $[C_nC_1Im]^+$ is more electron-poor than the C_{hetero} atoms of $[C_nC_1Pyrr]^+$ and $[C_nPy]^+$ when $[A]^-$ is common to all samples. For example, the binding energy of the C^2 component for $[C_8C_1Im][Tf_2N]$ is 287.7 eV,[2i] whereas the binding energies of C_{hetero} 1s for $[C_8C_1Pyrr][Tf_2N]$ and $[C_8Py][Tf_2N]$ were found to be 286.8[3a] and 287.0 eV, respectively. The similar binding energies of the C_{hetero} 1s in both $[C_8C_1Pyrr][Tf_2N]$ and $[C_8Py][Tf_2N]$ further supports the hypothesis that the C_{hetero} atoms of $[C_8C_1Pyrr][Tf_2N]$ and $[C_8Py][Tf_2N]$ are in very similar partial-charge environments. However, the binding energies of the C_{inter} atoms of $[C_8C_1Pyrr][Tf_2N]$ and $[C_8Py][Tf_2N]$ are very different from each other, that is, 285.5 and 286.1 eV respectively. This observation illustrates that the C_{inter} atoms for $[C_8Py][Tf_2N]$ are in a more electron-poor environment due to the sp^2 hybridisation and thus the delocalisation of the positive charge within the $[C_8Py]^+$ cation headgroup.

Pyrrolidinium-based ionic liquids have been investigated with a great deal of interest for the use in electrochemistry due to their greater stability when compared to imidazolium analogues, in terms of cation electrochemistry reduction.[27] Furthermore, pyridinium-based ionic liquids have also been reported to be more thermally stable when compared to imidazolium analogues.[10] The differences in stability can be correlated to the ease of removal of the C^2 proton within the imidazolium cation.[28] The XPS results here confirm that the C^2 carbon within the imidazolium cation is more electron-poor than any carbon atoms found within the pyrrolidinium and pyridinium cations. Therefore, in the electrochemistry study, the C^2 proton can be easily removed. These results support the conclusion that pyridinium-based ionic liquids are more stable than their imidazolium analogues.

3. Conclusions

We have successfully measured the XP spectra of a range of pyridinium-based ionic liquids, varying both the cation aliphatic chain length and the anion. The electronic environments of all the elements were identified. A reliable fitting model for the carbon 1s region of the pyridinium-based ionic liquids is pro-

duced taking into account the shake-up/off phenomena. The binding energy of the aliphatic carbon ($C_{aliphatic}$ 1s) moiety was determined with high confidence. The charge-corrected binding energies (absolute binding energies) for all the components could then be obtained.

Comparisons of the charge-corrected binding energies of the pyridinium cation's nitrogen atom, N_{cation} 1s (and also the carbon atoms directly bonded to nitrogen, C_{hetero} 1s) when the anion is varied were carried out. The binding energy for N_{cation} 1s decreases as the basicity of the anion increases, indicating that more charge is transferred from the anion to the cation for more basic anions such as bromide. In particular, mixtures of anions can be used to tune the electronic properties of ionic liquids.

A comparison of the binding energies of the cationic components for imidazolium-, pyrrolidinium- and pyridinium-based ionic liquids revealed significant differences. The charge on the nitrogen atoms in $[C_8Py][A]$ is significantly more electropositive than that on the nitrogen atoms in $[C_8C_1Im][A]$ but is found in a similar electronic environment as the nitrogen atoms in $[C_8C_1Pyrr][A]$. In addition, the C^2 carbon in imidazolium is more electropositive than any of the carbon atoms in the pyridinium cation. This observation agrees with the relative cathodic stability of the cations; pyridinium-based ionic liquids are generally more stable than their structurally related imidazolium analogues.

Acknowledgements

We would like to thank the EPSRC (EP/K005138/1) and Nature Science Foundation of Liaoning Province (2013020094) for financial support. PL acknowledges the EPSRC for the award of an ARF (EP/D073014/1). The authors are grateful to Dr. Emily F Smith for helpful discussions and critical advice.

Keywords: binding energy · fitting model · ionic liquids · pyridinium · X-ray photoelectron spectroscopy

[1] a) P. Wasserscheid, T. Welton, *Ionic Liquids in Synthesis* WILEY-VCH, Weinheim, **2007**; b) N. V. Plechkova, K. R. Seddon, *Chem. Soc. Rev.* **2008**, *37*, 123 – 150.

[2] a) E. F. Smith, I. J. Villar-Garcia, D. Briggs, P. Licence, *Chem. Commun.* **2005**, 5633 – 5635; b) J. M. Gottfried, F. Maier, J. Rossa, D. Gerhard, P. S. Schulz, P. Wasserscheid, H.-P. Steinrück, *Z. Phys. Chemie* **2006**, *220*, 1439 – 1453; c) S. Caporali, U. Bardi, A. Lavacchi, *J. Electron Spectrosc. Relat. Phenom.* **2006**, *151*, 4 – 8; d) O. Hofft, S. Bahr, M. Himmerlich, S. Krischok, J. A. Schaefer, V. Kempter, *Langmuir* **2006**, *22*, 7120 – 7123; e) C. Kolbeck, M. Killian, F. Maier, N. Paape, P. Wasserscheid, H.-P. Steinrück, *Langmuir* **2008**, *24*, 9500 – 9507; f) V. Lockett, R. Sedev, C. Bassell, J. Ralston, *Phys. Chem. Chem. Phys.* **2008**, *10*, 1330 – 1335; g) T. Cremer, C. Kolbeck, K. R. J. Lovelock, N. Paape, R. Wölfel, P. S. Schulz, P. Wasserscheid, H. Weber, J. Thar, B. Kirchner, F. Maier, H.-P. Steinrück, *Chem. Eur. J.* **2010**, *16*, 9018 – 9033; h) K. R. J. Lovelock, I. J. Villar-Garcia, F. Maier, H.-P. Steinrück, P. Licence, *Chem. Rev.* **2010**, *110*, 5158 – 5190; i) I. J. Villar-Garcia, E. F. Smith, A. W. Taylor, F. Qiu, K. R. J. Lovelock, R. G. Jones, P. Licence, *Phys. Chem. Chem. Phys.* **2011**, *13*, 2797 – 2808; j) B. B. Hurisso, K. R. J. Lovelock, P. Licence, *Phys. Chem. Chem. Phys.* **2011**, *13*, 17737 – 17748; k) I. J. Villar-Garcia, K. R. J. Lovelock, S. Men, P. Licence, *Chem. Sci.* **2014**, *5*, 2573 – 2579.

[3] a) S. Men, K. R. J. Lovelock, P. Licence, *Phys. Chem. Chem. Phys.* **2011**, *13*, 15244 – 15255; b) S. Men, B. B. Hurisso, K. R. J. Lovelock, P. Licence, *Phys. Chem. Chem. Phys.* **2012**, *14*, 5229 – 5238.

[4] a) B. K. Ni, Q. Y. Zhang, A. D. Headley, *Tetrahedron Lett.* **2008**, *49*, 1249 – 1252; b) L. Ford, F. Atefi, R. D. Singer, P. J. Scammells, *Eur. J. Org. Chem.* **2011**, 942 – 950.

[5] M. Mahrova, F. Pagano, V. Pejakovic, A. Valea, M. Kalin, A. Igartua, E. Tojo, *Tribol. Int.* **2015**, *82*, 245 – 254.

[6] N. M. Yunus, M. I. A. Mutalib, Z. Man, M. A. Bustam, T. Murugesan, *Chem. Eng. J.* **2012**, *189*, 94 – 100.

[7] B. Bittner, R. J. Wrobel, E. Milchert, *J. Chem. Thermodyn.* **2012**, *55*, 159 – 165.

[8] a) N. M. Yunus, M. I. A. Mutalib, Z. Man, M. A. Bustam, T. Murugesan, *J. Chem. Thermodyn.* **2010**, *42*, 491 – 495; b) C. Cadena, Q. Zhao, R. Q. Snurr, E. J. Maginn, *J. Phys. Chem. B* **2006**, *110*, 2821 – 2832.

[9] M. Vilas, M. A. A. Rocha, A. M. Fernandes, E. Tojo, L. Santos, *Phys. Chem. Chem. Phys.* **2015**, *17*, 2560 – 2572.

[10] L. G. Sanchez, J. R. Espel, F. Onink, G. W. Meindersma, A. B. de Haan, *J. Chem. Eng. Data* **2009**, *54*, 2803 – 2812.

[11] a) J. M. Crosthwaite, M. J. Muldoon, J. K. Dixon, J. L. Anderson, J. F. Brennecke, *J. Chem. Thermodyn.* **2005**, *37*, 559 – 568; b) A. Deyko, K. R. J. Lovelock, J.-A. Corfield, A. W. Taylor, P. N. Gooden, I. J. Villar-Garcia, P. Licence, R. G. Jones, V. G. Krasovskiy, E. A. Chernikova, L. M. Kustov, *Phys. Chem. Chem. Phys.* **2009**, *11*, 8544 – 8555.

[12] a) E. F. Smith, F. J. M. Rutten, I. J. Villar-Garcia, D. Briggs, P. Licence, *Langmuir* **2006**, *22*, 9386 – 9392; b) K. R. J. Lovelock, E. F. Smith, A. Deyko, I. J. Villar-Garcia, P. Licence, R. G. Jones, *Chem. Commun.* **2007**, 4866 – 4868; c) K. R. J. Lovelock, C. Kolbeck, T. Cremer, N. Paape, P. S. Schulz, P. Wasserscheid, F. Maier, H.-P. Steinrück, *J. Phys. Chem. B* **2009**, *113*, 2854 – 2864.

[13] S. Men, K. R. J. Lovelock, P. Licence, *RSC Adv.* **2015**, *5*, 35958 – 35965.

[14] A. W. Taylor, S. Men, C. J. Clarke, P. Licence, *RSC Adv.* **2013**, *3*, 9436 – 9445.

[15] J. G. Huddleston, A. E. Visser, W. M. Reichert, H. D. Willauer, G. A. Broker, R. D. Rogers, *Green Chem.* **2001**, *3*, 156 – 164.

[16] A. W. Taylor, K. R. J. Lovelock, A. Deyko, P. Licence, R. G. Jones, *Phys. Chem. Chem. Phys.* **2010**, *12*, 1772 – 1783.

[17] D. Briggs, J. T. Grant, *Surface Analysis by Auger and X-ray Photoelectron Spectroscopy*, IMPublications, Manchester **2003**.

[18] C. Kolbeck, T. Cremer, K. R. J. Lovelock, N. Paape, P. S. Schulz, P. Wasserscheid, F. Maier, H.-P. Steinrück, *J. Phys. Chem. B* **2009**, *113*, 8682 – 8688.

[19] C. D. Wagner, L. E. Davis, M. V. Zeller, J. A. Taylor, R. H. Raymond, L. H. Gale, *Surf. Interface Anal.* **1981**, *3*, 211 – 225.

[20] G. Beamson, D. Briggs, *Mol. Phys.* **1992**, *76*, 919 – 936.

[21] J. F. Moulder, W. F. Stickle, P. E. Sobol, K. D. Bomben, *Handbook of X-ray Photoelectron Spectroscopy: a reference book of standard spectra for identification and interpretation of XPS data*, Physical Electronics, **1995**.

[22] a) V. Yarzhemsky, V. I. Nefedov, M. B. Trzhaskovskaya, I. M. Band, R. Szargan, *J. Electron Spectrosc. Relat. Phenom.* **2002**, *123*, 1 – 10; b) S. Svensson, B. Eriksson, N. Martensson, G. Wendin, U. Gelius, *J. Electron Spectrosc. Relat. Phenom.* **1988**, *47*, 327 – 384.

[23] a) D. Briggs, G. Beamson, *Anal. Chem.* **1993**, *65*, 1517 – 1523; b) B. Sjogren, S. Svensson, A. N. Debrito, N. Correia, M. P. Keane, C. Enkvist, S. Lunell, *J. Chem. Phys.* **1992**, *96*, 6389 – 6398.

[24] T. Robert, *Chem. Phys.* **1975**, *8*, 123 – 135.

[25] T. Cremer, M. Killian, J. M. Gottfried, N. Paape, P. Wasserscheid, F. Maier, H.-P. Steinrück, *ChemPhysChem* **2008**, *9*, 2185 – 2190.

[26] F. Maier, T. Cremer, C. Kolbeck, K. R. J. Lovelock, N. Paape, P. S. Schulz, P. Wasserscheid, H.-P. Steinrück, *Phys. Chem. Chem. Phys.* **2010**, *12*, 1905 – 1915.

[27] R. Wibowo, S. E. W. Jones, R. G. Compton, *J. Chem. Eng. Data* **2010**, *55*, 1374 – 1376.

[28] a) M. C. Kroon, W. Buijs, C. J. Peters, G. J. Witkamp, *Green Chem.* **2006**, *8*, 241 – 245; b) P. Bonhôte, A. P. Dias, N. Papageorgiou, K. Kalyanasundaram, M. Grätzel, *Inorg. Chem.* **1996**, *35*, 1168 – 1178.

Received: March 17, 2015
Published online on May 7, 2015

